

ULTRAVIOLET MEASUREMENTS IN PLANETARY  
ATMOSPHERES \*

Wm. G. Fastie

The Johns Hopkins University  
Baltimore, Maryland 21218

ABSTRACT

The impact of the latest optical and electronic component developments on far ultraviolet rocket spectrophotometry is discussed. Results of some recent experiments studying earth airglow and aurorae are reviewed. It is shown that weaker spectral features can be measured in the region 1100 to 3000 Å than at any longer wavelength.

N66 38722

FACILITY FORM 605

(ACCESSION NUMBER)  
29  
(PAGES)  
CR-78485  
(NASA CR OR TMX OR AD NUMBER)

(THRU)  
1  
(CODE)  
13  
(CATEGORY)

GPO PRICE \$ \_\_\_\_\_

CFSTI PRICE(S) \$ \_\_\_\_\_

Hard copy (HC) \$2.00

Microfiche (MF) 1.50

# ULTRAVIOLET MEASUREMENTS IN PLANETARY ATMOSPHERES

## I. INTRODUCTION

The first rocket measurements of ultraviolet emissions in the earth's atmosphere were made less than ten years ago. During the present decade planetary fly-by vehicles will carry U. V. instruments to study Venus and Mars. Most of the components which will make up these instruments did not exist ten years ago, and represent several orders of magnitude improvement in detectability during that period. These improvements in ultraviolet technology have been as dramatic as infrared instrumentation advances were in the 1940 to 1950 decade. To emphasize this point, it will be shown later that it is possible to measure the spectrum of a weaker source in the wavelength region below 3000 Å with uncooled detectors than at any longer wavelength.

The ultraviolet spectral region is particularly important for studying the ionospheric and exospheric regions of planetary atmospheres for a number of reasons. Almost all of the ground state resonance lines of atomic species are in this region, and resonance reradiation of solar U. V. flux is an important upper atmospheric reaction. Almost all of the ions and neutral molecules in the ionosphere absorb and fluoresce in the U. V. The ionospheric processes of dissociation, recombination and charge exchange produce emission in this region. Collisions between atmospheric species and high energy particles, such as solar protons, auroral electrons and photoelectrons produced by extreme ultraviolet photo ionization, have a high cross section for emission

of U. V. radiation. The U. V. measurements which permit all of the above processes to be studied provide an important tool for studying planetary atmospheres. The possibility provided by rockets to observe these processes on a scale and at pressures not available in the laboratory permits basic atomic and molecular studies not previously possible.

The purpose of this paper is to describe the techniques and optical components which are presently employed in U. V. space measurements and to present some of the experimental data which have been obtained. The instrumentation to be described is applicable to all spectral ranges above the present cutoff wavelength of lithium fluoride windows at about 1050 Å.

## II. ENERGY RELATIONSHIPS

The signal in photoelectrons delivered to a photometer detector (Fig. 1) is given by the equation

$$S_{pe} = B_s^s \frac{A_c A_d}{F^2} Q T \quad (1)$$

where  $B_s^s$  is the brightness in photons /cm<sup>2</sup>/sec/ster.

$A_c$  is the area of the collector.

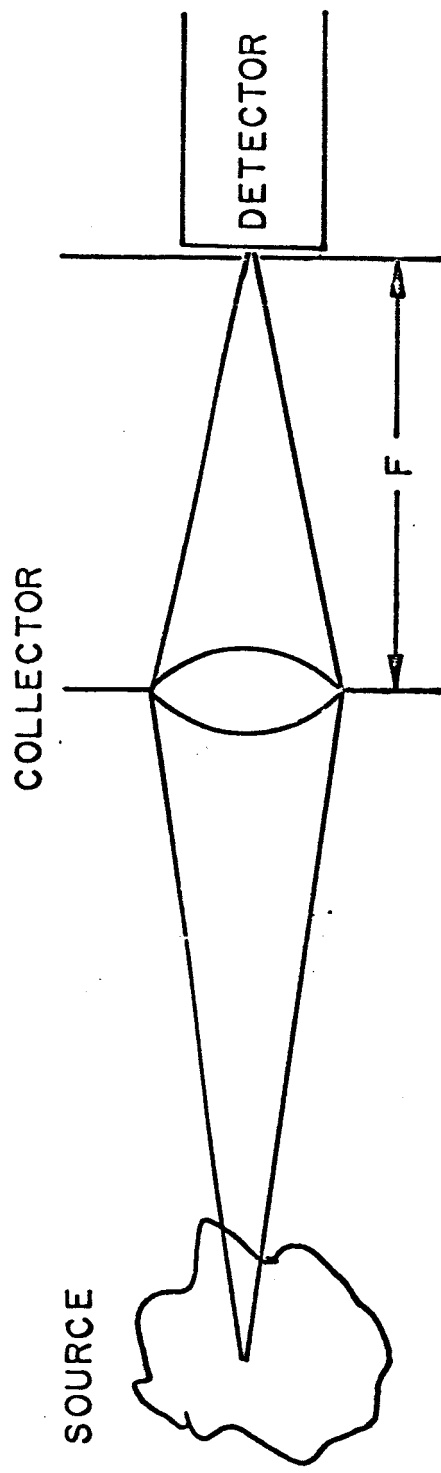
$A_d$  is the illuminated area of the detector.

$F$  is the distance from the detector to the collector.

$Q$  is the quantum efficiency of the detector.

$T$  is the transmission of the system.

When applied to a mirror grating spectrophotometer used at or near the Littrow position ( $\alpha = \beta$ ) the grating can be considered to be the collector and the slit defines the detector area; equation (1)



becomes

$$S_{pe} = B_s^s A_g \frac{\cos \alpha LW}{F^2} Q R^2 B_g \quad (2)$$

where  $A_g \cos \alpha$  is the projected grating area ( $\alpha$  is the angle of incidence or diffraction).

$L$  is the slit length.

$W$  is the slit width.

$F$  is the focal length of the spectrometer.

$R$  is the mirror reflectivity.

$B_g$  is the grating efficiency.

In a Littrow or near Littrow grating spectrophotometer, the projected area of the grating decreases by  $\cos \alpha$  as  $\alpha$  increases, but the dispersion increases by  $\tan \alpha$  with increasing  $\alpha$ , with the result that the slit width can be increased as  $\alpha$  increases to maintain a constant spectral band pass and there is a net gain in signal with increasing  $\alpha$  ( $\cos \alpha \tan \alpha = \sin \alpha$ ). Furthermore, as the focal length increases, the slit width can be increased proportionately for constant spectral band pass ( $w/f = c$ ). Thus equation (2) can be written

$$S_{pe} = c B_s^s A_g \sin \alpha \frac{L}{F} Q R^2 B_g \quad (3)$$

### III. DEFINITION OF BRIGHTNESS UNIT

In studying emission of extended three dimension optically thin sources, the important parameter is the number of emitting atoms per square centimeter column in the observing direction. Each cubic centimeter of the source emits over  $4\pi$  solid angle. The unit of brightness used almost universally for upper atmospheric

studies is the Rayleigh which is one millionth the number of photons emitted per sq. cm. col. The apparent surface brightness ( $B_s^s$ ) of an extended three dimensional source has a simple geometrical relation to the Rayleigh

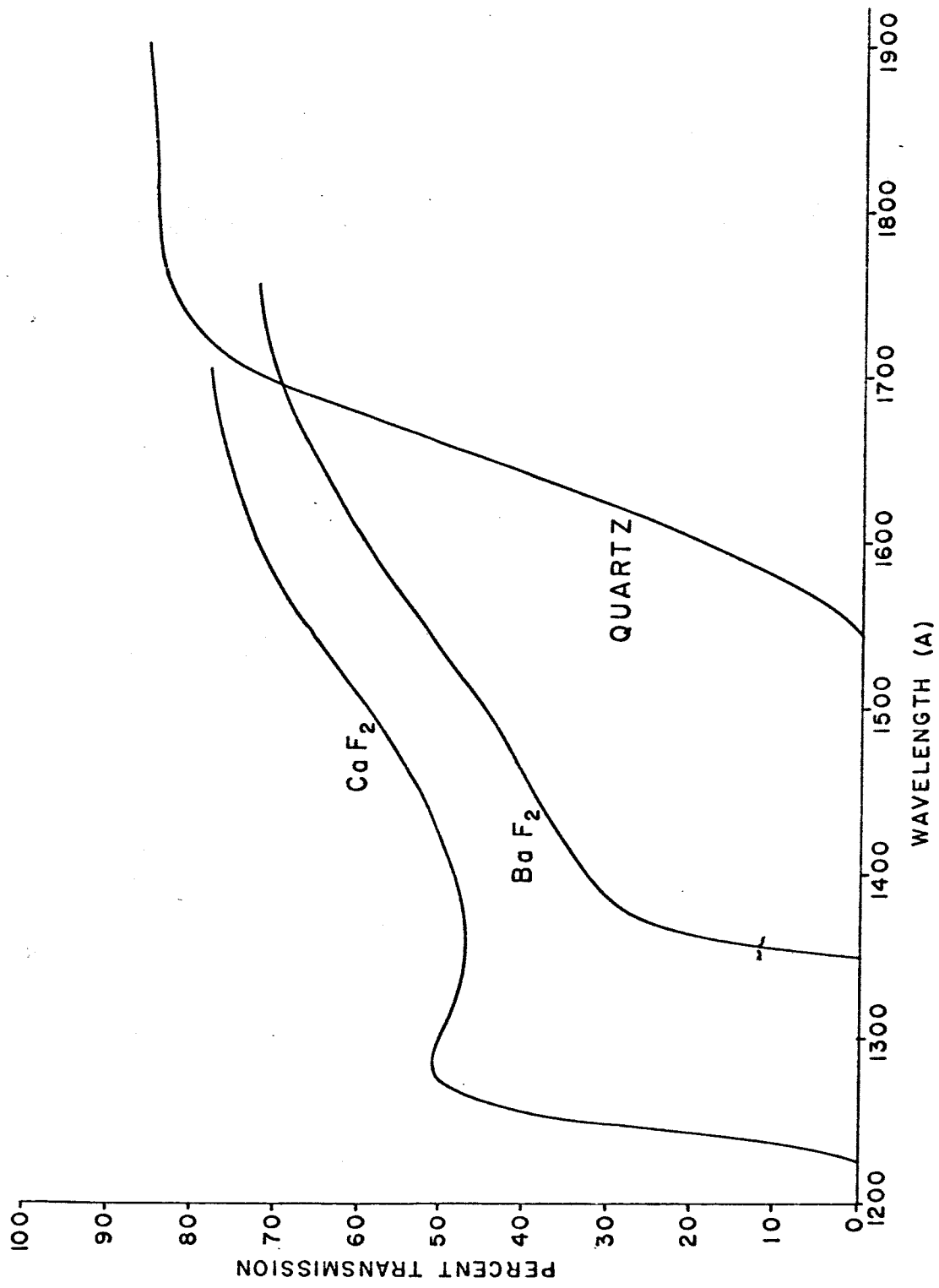
$$B_s^s = \frac{R}{4 \pi \times 10^6} \quad (4)$$

where  $B_s^s$  is photons/cm<sup>2</sup>/ sec/ster.

R is Rayleighs (10<sup>6</sup> photon/sq. cm. col.)

#### IV. DIFFERENTIAL FILTER PHOTOMETRY BELOW 2000 Å

At the present time no efficient narrow band filters exist for the spectral region between 1050 and 2000 Å. There are a number of window materials, however, which have sharp short wavelength cutoffs at wavelengths longer than the 1050 Å cutoff of lithium fluoride. Fig. 2 shows the transmission characteristics of these materials. By using a multiple photometer, each with a different window or a single detector with a rotating filter wheel, the region 1050 to 1250 Å, 1250 to 1350 Å, and 1350 to 1600 Å can be isolated. By using a quartz window with a CsI photomultiplier tube the region 1600 to 1900 Å can be isolated. Although the differential filtering technique provides poor resolution, there are many problems in planetary studies for which they are useful. For example, in the earth's nightglow and day airglow, the major emission in the region 1050 to 1250 Å is the Ly  $\alpha$  line of atomic hydrogen at 1216 Å and the major emission in the region 1250 to 1350 Å are the three resonance lines of atomic oxygen at 1302, 1304, and 1306 Å. This type of instrumentation has been used to study these emissions in the earth's atmosphere. A multiple photometer employing these filters will be incorporated in the 1967 Venus fly-by



vehicle to study these emissions in the upper regions of the Venusian atmosphere.  $\neq$

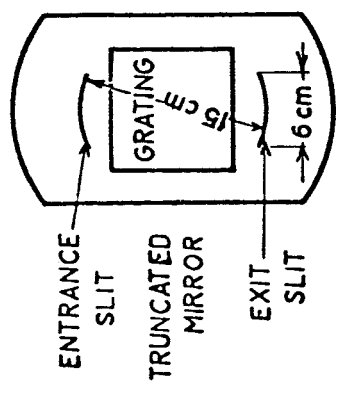
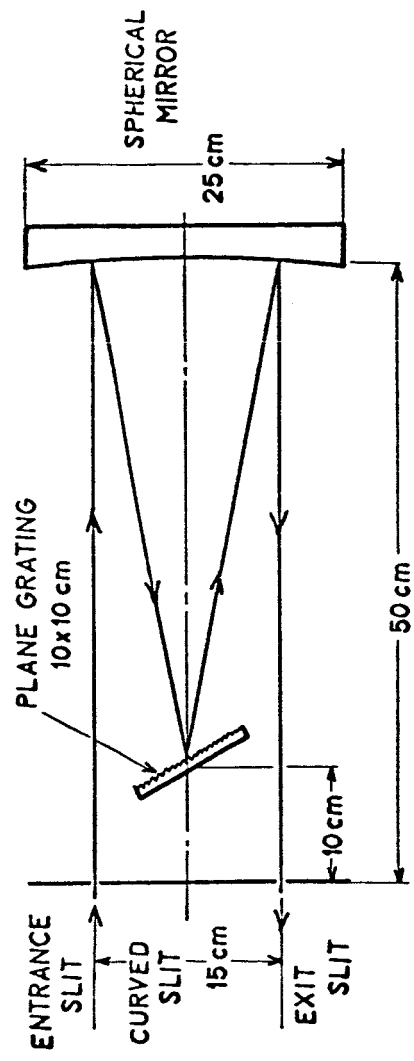
## V. EBERT SPECTROPHOTOMETER

The properties which have made the Ebert spectrometer the most widely used instrument for rocket and satellite studies have been described in great detail <sup>1,2</sup> and will only be briefly reviewed. The system shown in Fig. 3 can employ very long slits without loss of resolution and thus, can provide a maximum output signal. In practice, values of  $L/F$  of 0.2 have been employed. In addition, this plane grating single spherical mirror folded optical system is very rugged and can be designed so that misalignment of the optical components in flight is practically impossible. Although for optimum resolution, the Ebert system should not be used below  $f/10$  or  $f/15$ , a resolution of one or two angstrom units can be obtained when the  $f$  number is as low as  $f/4$ . Equation (3) shows that the signal is independent of the  $f$  number, but the low  $f$  number capability of the Ebert system is important because of the dimensional limitations of spacecraft.

## VI. OPTICAL COMPONENTS

Referring again to equation (3), the discovery by Haas <sup>3</sup> of high reflectivity mirror coatings for the region below 2000 Å was an important development for this region. A value of  $R^2$  of 0.6 at 1200 Å is now routine with commercially available mirrors of Al overcoated with magnesium fluoride. Another important contribution was the work of the late David Richardson at Bausch and Lomb Optical Company in developing high efficiency gratings for





the far ultraviolet. The availability of 3600 groove/mm (90,000 lines/inch) gratings as compared to the 600 groove/mm gratings previously available for this region represents a sixfold increase in sensitivity because of the increase in  $\sin \alpha$  (Eq. 3). Furthermore, these finely ruled gratings are quite efficient, having blazes of 25 to 30% at wavelengths as short as 1216 Å, and are available in sizes up to 100 sq. cm. ruled area.

The development of high quantum efficiency photomultiplier tubes with lithium fluoride windows and high work function photocathodes has been another vital facet of far U. V. instrumentation. For example, photocathodes of caesium iodide have a quantum efficiency of 10% at 1200 Å but have a work function of about 5 volts with the result that they are completely insensitive beyond 2000 Å (solar blind) and are almost completely free of spontaneous emission of thermal electrons even at 300° K, at which temperature the typical dark current is a few electrons per second. The insensitivity of these detectors to the predominating longer wavelength solar radiation makes it possible to detect very weak far U. V. signals without the disturbance of long wavelength scattered light.

Referring one final time to equation (3), it can be seen from the numbers quoted above that sensitivity capability in the far U. V. is entirely comparable to that available in the visible region. That is,  $A_g$ ,  $\alpha$ ,  $L/F$ ,  $Q$ ,  $R$ , and  $B_g$  are comparable numbers in the visible and ultraviolet. However, photomultiplier tubes sensitive to visible light must be cooled to approach the performance available with solar blind tubes. For example, in our rocket experiments we routinely make U. V. measurements in 100 milliseconds of signals as small as 100 photoelectrons per second.

## VII. MEASURING CIRCUITS

One of the advantages of negligible dark currents is that conventional pulse counting circuits can be employed. Far U. V. photomultiplier tubes can be operated at gains up to  $10^7$  where the dark current is typically below  $10^{-11}$  amperes and a signal of 100 photoelectrons per second produces a current of  $1.6 \times 10^{-10}$  amperes. Pulses of  $10^7$  electrons can be measured with the most rudimentary pulse counting circuitry or alternatively currents of  $10^{-10}$  amperes can be measured in analog fashion with solid state electrometer circuitry. Solid state DC to DC converters can be designed with highly stabilized outputs of a few kilovolts to provide the high gain the photomultiplier tubes require. Pulse counting devices or analog amplifiers require only a few milliwatts of electrical power and DC to DC converters require only a fraction of a watt to sensitize the photomultiplier tube. All of this equipment suitable for rocket or satellite use and compatible with telemetry circuitry is now commercially available or alternatively can be built by a minimal electronics facility.

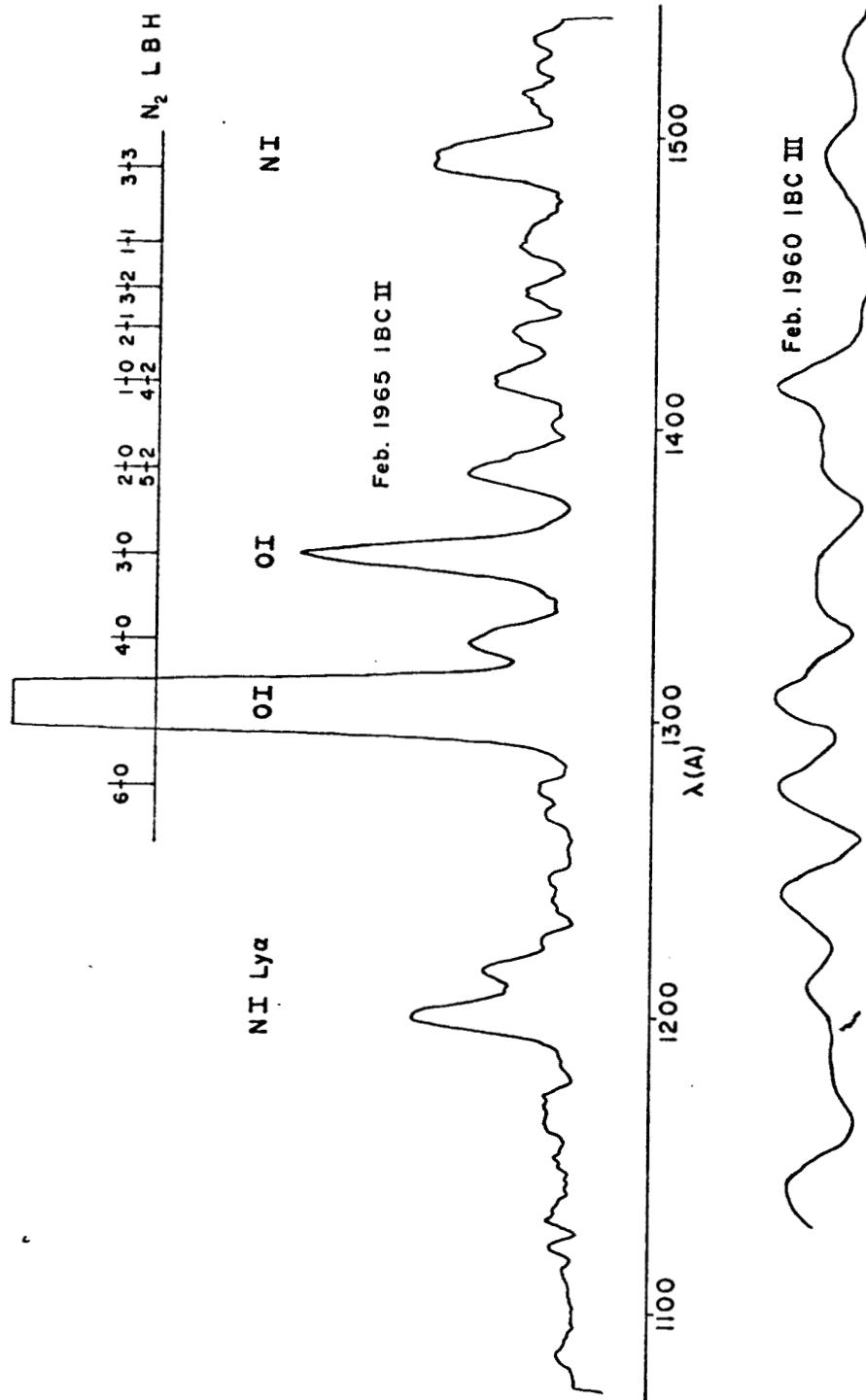
In all of our measurements we have employed analog circuitry but have transmitted and received the output signals with a time resolution of a few milliseconds. The purpose of this mode of operation was to make it easy to recognize occasional false signals arising from cosmic rays, coronal discharge from the tube face or internal breakdown in the photomultiplier tube. An unanticipated result of this technique has been an extension of the dynamic range of the telemetry measuring circuitry which is nominally 100. When the analog signal goes below the limits of the telemetry circuitry, individual pulses are observable on the telemetry record. We have thus on occasion measured light signals as low as five photoelectrons per second with linear circuitry for which the full scale analog signal was 50,000 photoelectrons per second.

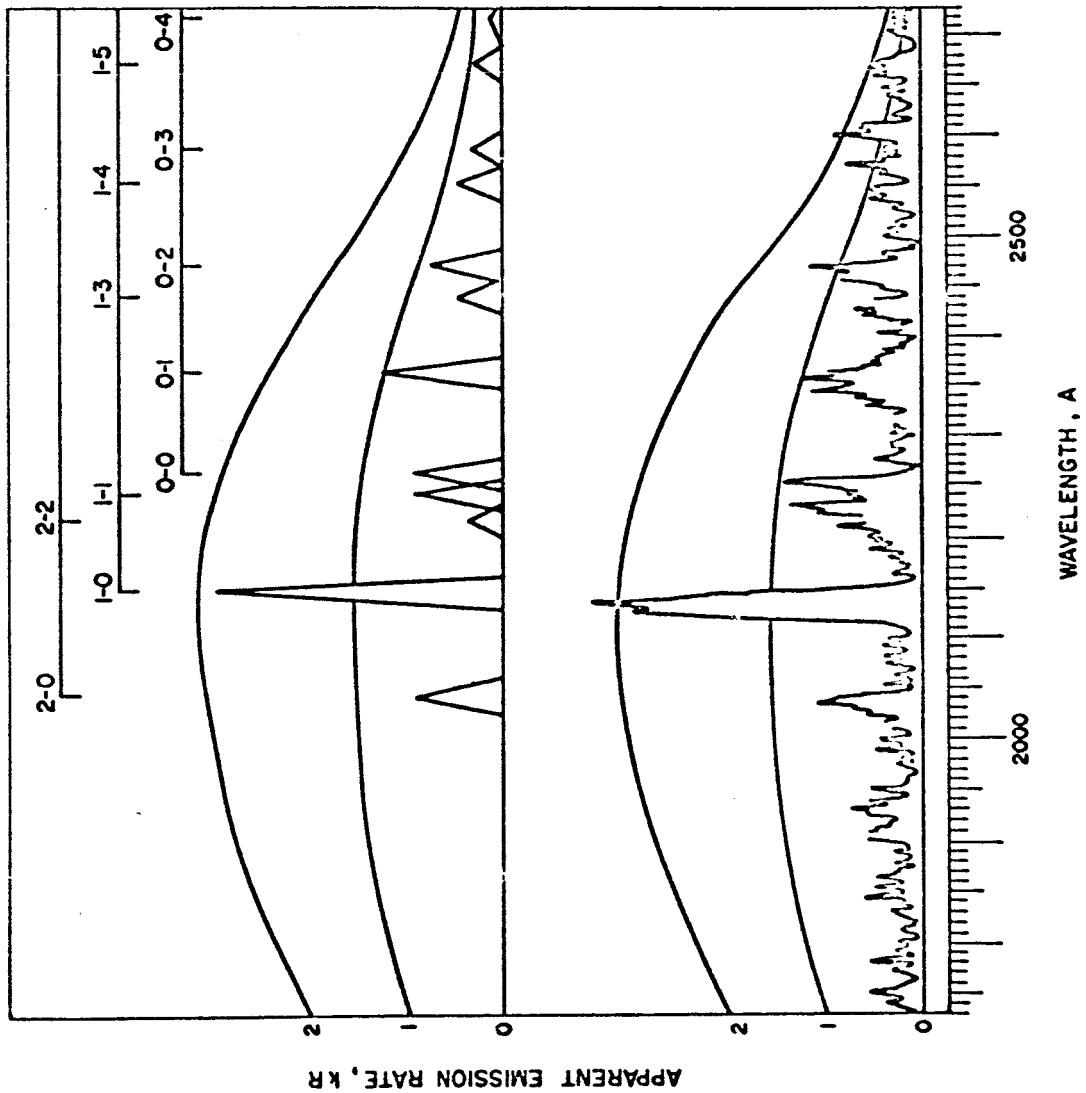
### VIII. EXPERIMENTAL RESULTS

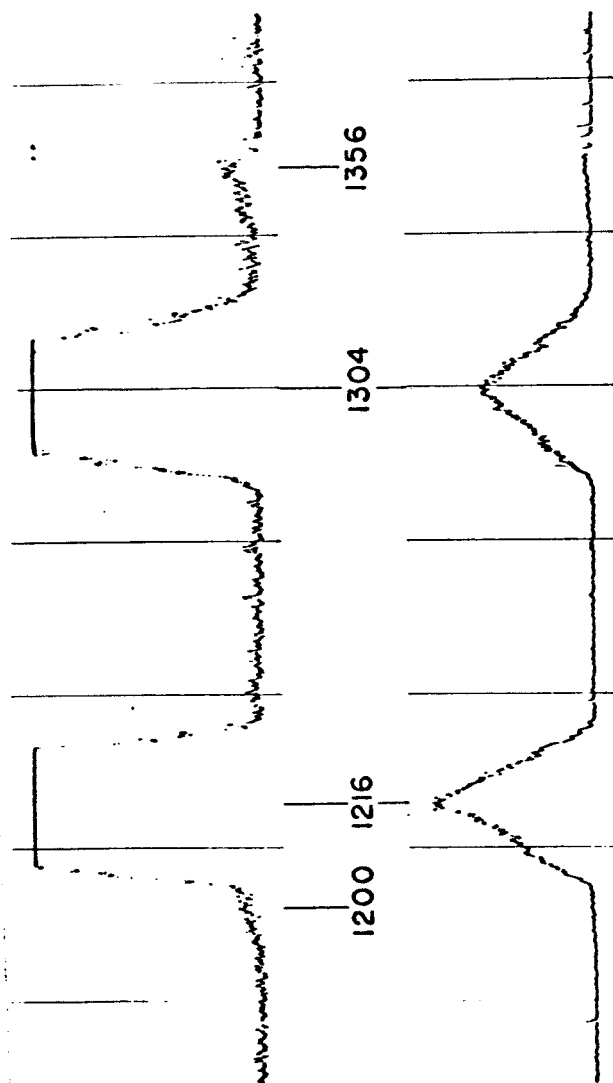
In 1960 we obtained the first far U. V. auroral spectrum <sup>4, 5</sup> using a 1200 groove/mm grating and a blue sensitive photomultiplier tube coated with sodium salicylate. In 1965 we repeated the experiment with the presently available gratings and detectors described in the previous sections. Fig. 4 shows the two spectra obtained and clearly illustrates the dominant theme of this discussion. Both spectra were obtained in the same observation time and with the same spectral resolution. The 1960 aurora was 10 times as bright as the 1965 aurora.

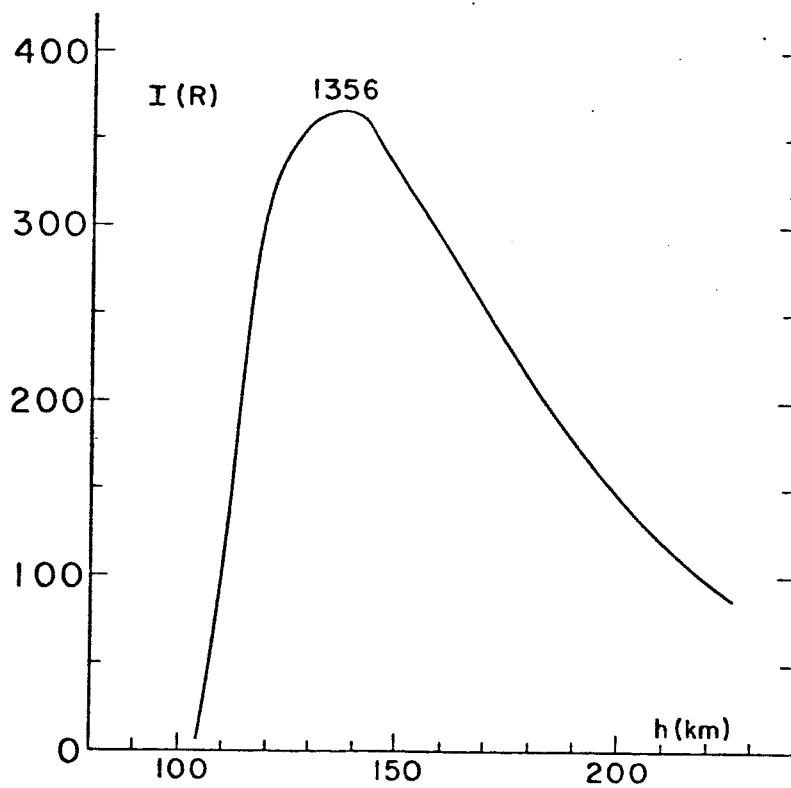
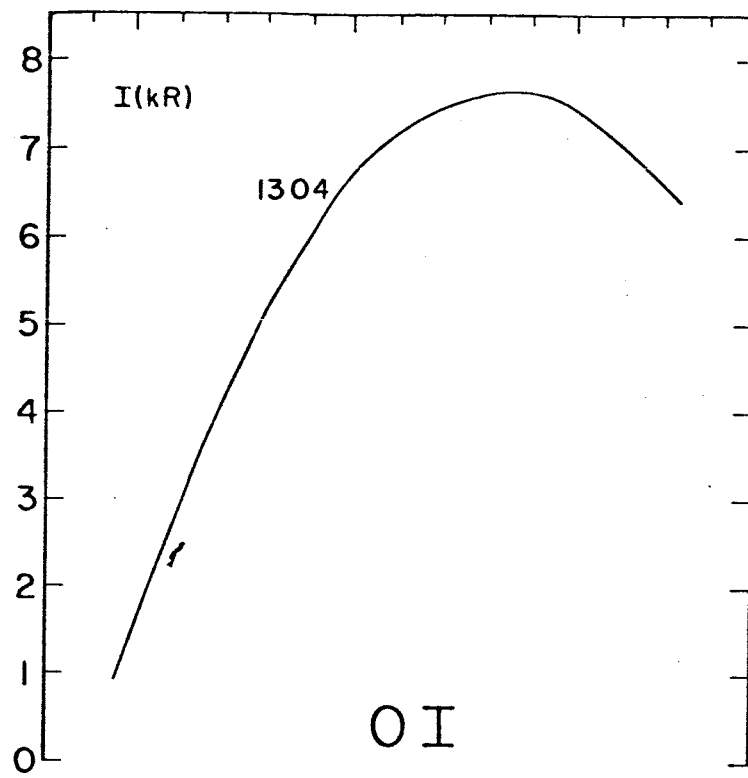
Fig. 5 is the spectrum of nitric oxide obtained by Barth <sup>6</sup>. This emission is produced by fluorescence under solar U. V. flux. The spectrum shown represents one second of observation time from an Aerobee rocket.

Fig. 6 shows a spectrum of the far U. V. day airglow <sup>7</sup> obtained with an Aerobee rocket. There are 4 spectral features identifiable in this figure which is a copy of an unretouched telemetry record. The atomic nitrogen resonance line at 1200 Å is a wing on the dominating Ly  $\alpha$  atomic hydrogen resonance line. The unresolved resonance lines of atomic oxygen at 1304 Å is the other bright feature. The forbidden lines of atomic oxygen at 1356 Å also appear. Fig. 7 shows the altitude profile of the two oxygen features. These data have produced new understanding of the processes which create these emissions in the upper atmosphere and of the manner in which these radiations are transported in the planetary atmosphere.









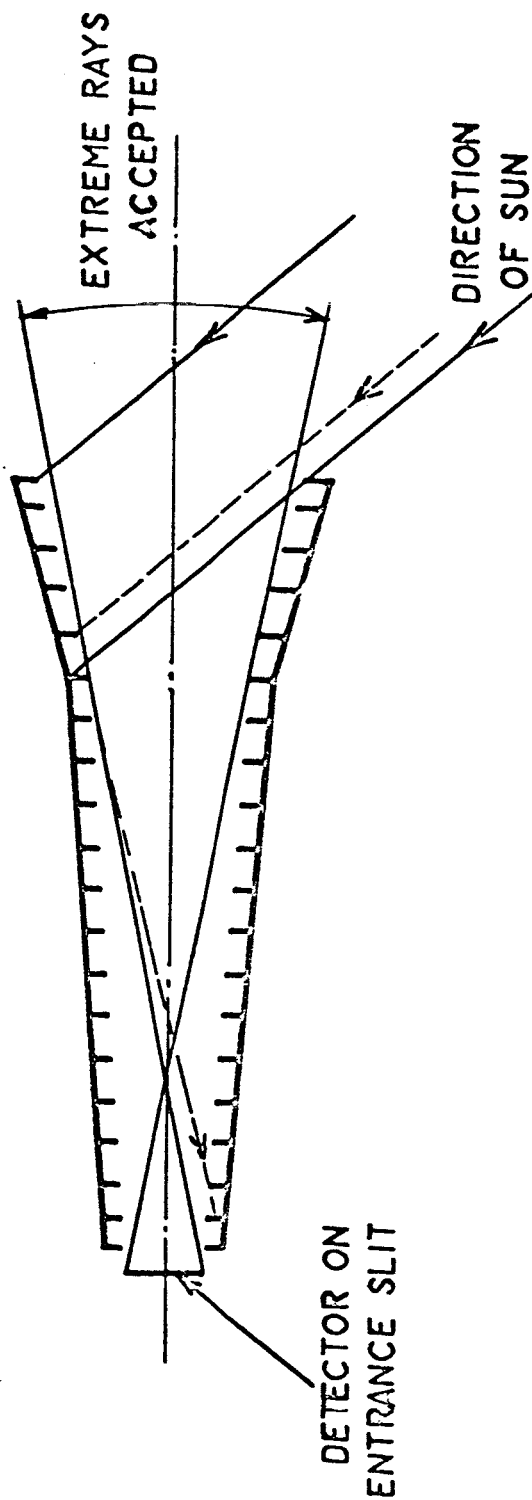


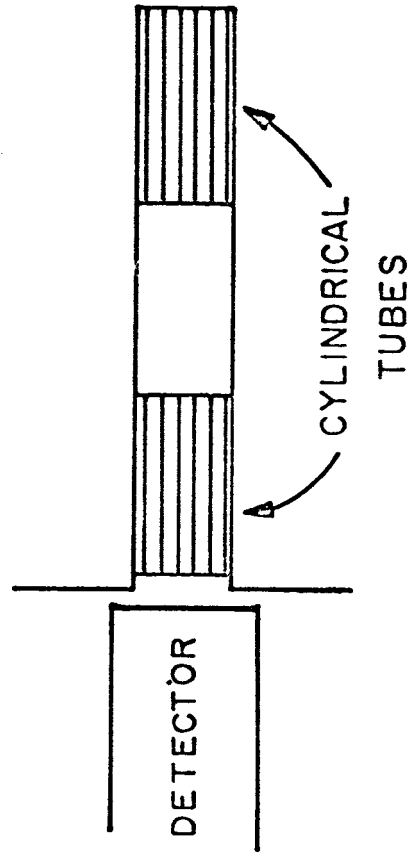
## IX. COLLECTING OPTICS

In studying night airglow and aurora in the earth's atmosphere, no collecting optics are needed because the source is so large, and no baffling of the entrance slit is required. In day airglow measurements, the optic axis of the spectrometer or photometer can be at large angles to the sun, but even so scattering of solar radiation from the slit jaws or from baffle edges produces large false signals. Fig. 8 shows a double baffle which has been used to reduce the effect of solar scattering. The outer baffle is arranged to shade the inner baffle, and solar radiation scattered from the outer baffle must scatter again from the inner baffle in order to reach the entrance slit or detector. The angle of the inner baffle is adjusted for spectrometer applications so that doubly scattered light which reaches the entrance slit must be scattered again by the entrance slit jaws or the Ebert mirror in order to reach the exit slit.

Another baffling technique which has been used for day airglow measurements employs field of view limiters. In its simplest form two bundles of thin walled cylinders are placed in front of a detector as shown in Fig. 9 to provide very high transmission only over a very narrow viewing angle.

When airglow measurements must be made at small angles to a bright object, a collecting telescope is required to reject radiation from the object. For example, satellite observations of the horizon airglow, planetary fly-by measurements, or measurement of emissions in the solar corona, require auxiliary focusing elements. The occulting telescope, or coronagraph optical system shown in Fig. 10 has been used in these applications. The image of the planet or solar surface is formed in space at the focal plane of



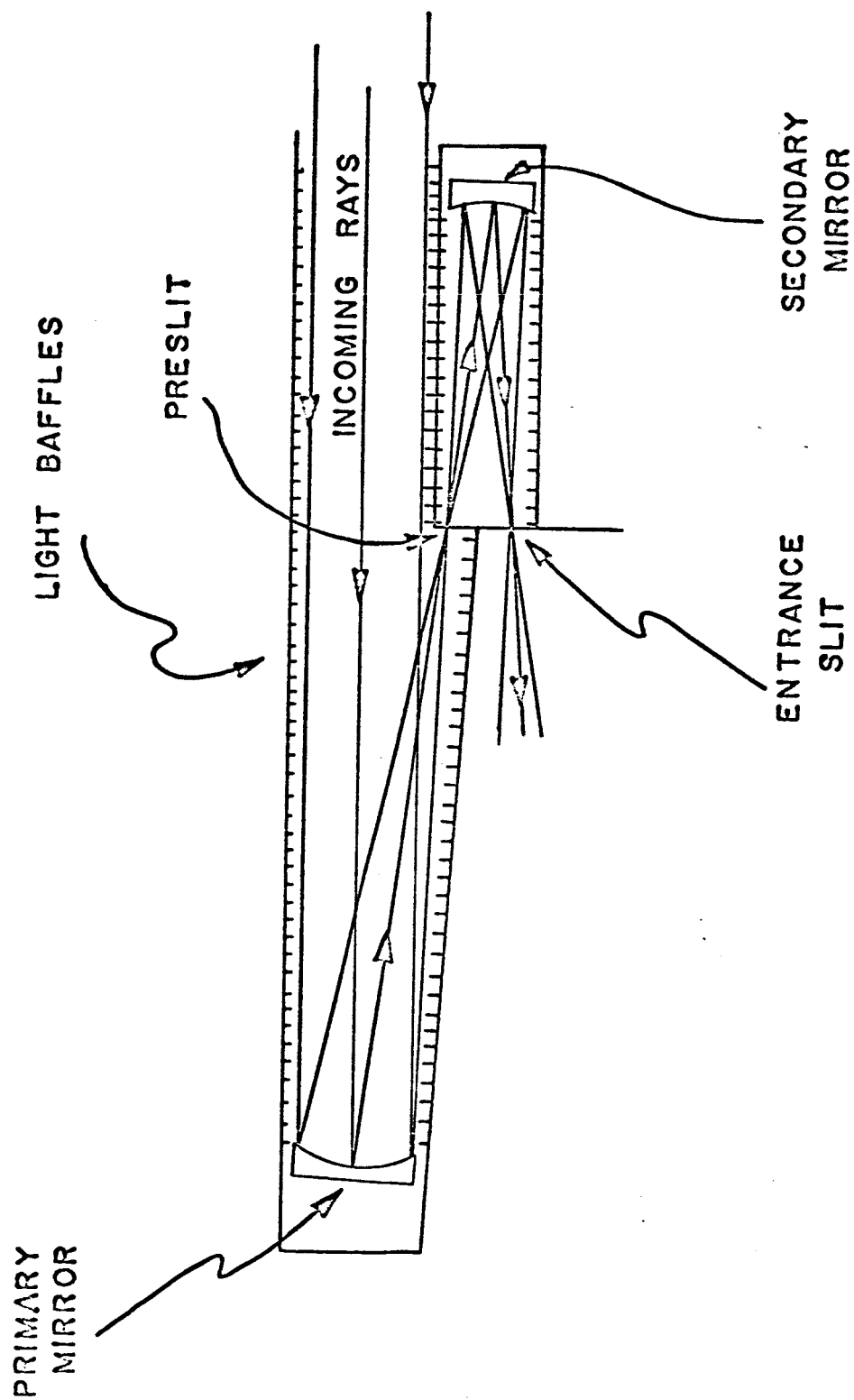


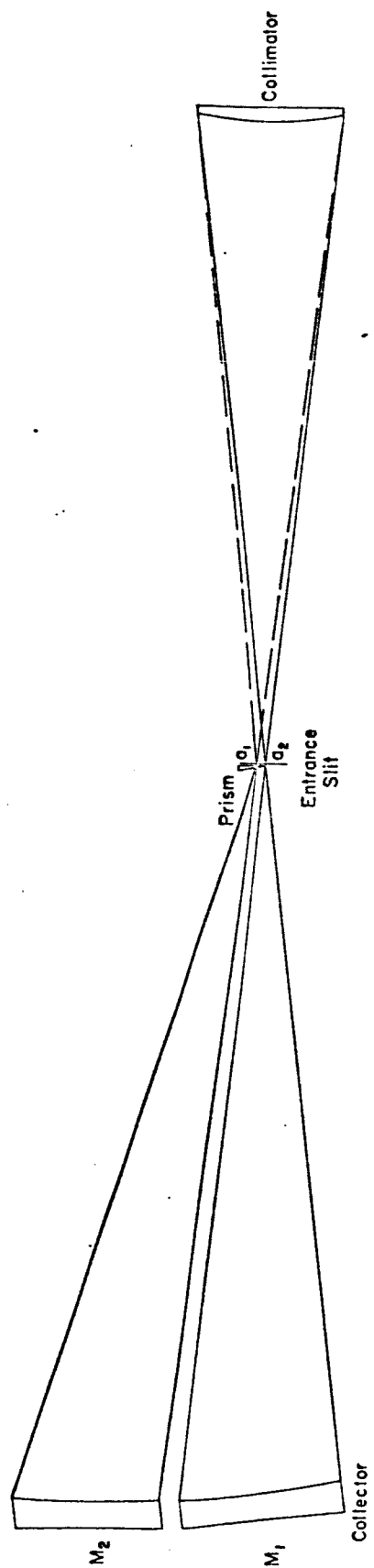
END VIEW

the primary mirror and this radiation is thus returned to outer space. Radiation scattered from the baffles in the primary telescope must scatter from the occulting slit or from the baffles in the secondary mirror system in order to enter the spectrometer. The most serious scatter signal from this system is the radiation scattered from the primary mirror through the pre slit.

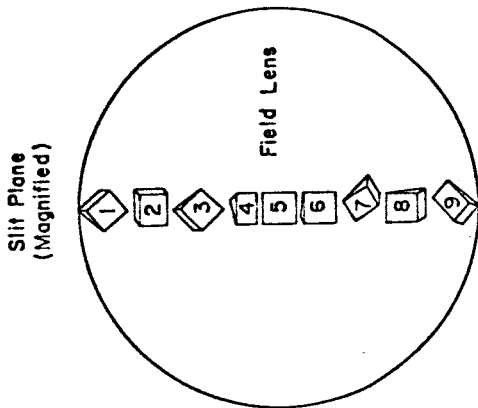
There are many planetary atmospheric measurements and astrophysical measurements in which the source is not extended and which cannot take advantage of the long slit capabilities of the Ebert system. For these applications, the collecting system<sup>8</sup> shown in Fig. 11 may be employed. Each collecting mirror forms an image of the same part of the sky or of the same astronomical object on the entrance slit. The  $f$  number of each mirror is sufficient to fill the optics of the spectrometer. At the entrance slit a small prism redirects the radiation from each mirror along the optic axis of the spectrometer. Fig. 12 shows a system employing nine mirrors to provide a nine-fold increase in signal strength. Each of the nine mirrors also images other parts of the sky or other astronomical objects on other parts of the entrance slit, but the redirecting prisms do not send this radiation to the diffraction grating. This imaging device has not been used to date.

The combination of the advanced techniques now available for ultraviolet measurements and the multitude of planetary problems which can be attacked by these techniques will produce an expanded program in this area in the next decade. Application of the techniques to the study of stellar atmospheres and galactic atmospheres has already begun.





Collector Mirror Plane		
1	2	3
4	5	6
7	8	9



Prisms 2, 4, 6, and 8 have angle  $\alpha$   
 5 has angle  $\phi$   
 1, 3, 7, and 9 have angle  $1.4\alpha$

Collimator Plane		
7	8	9
Peripheral Areas Collect Unwanted Radiation From Nearby Sources.		
4	6	
Collimator Collects All Rays From All 9 Images Of Source.		
1	2	3

## FOOTNOTES

- \* Presented at the Aerospace Techniques Symposium,  
Cambridge, Massachusetts, July 8, 1966.
- ≠ C. A. Barth, University of Colorado, is preparing this  
experiment.



## REFERENCES

1. Wm. G. Fastie, J. Opt. Soc. Am. 42, 641 (1952).
2. Wm. G. Fastie, J. Quant. Spec. Radiat. Transfer 3, 505 (1963).
3. G. Haas and R. Tousey, J. Opt. Soc. Am. 9, 593 (1959).
4. Wm. G. Fastie, etal, Ann. de Geophysique 17, 109 (1961).
5. H. M. Crosswhite, etal, J. Opt. Soc. Am. 52, 643 (1962).
6. C. A. Barth, J. Geophys. Res. 69, 3301 (1964).
7. Wm. G. Fastie, etal, J. Geophys. Res. 69, 4129 (1964).
8. Wm. G. Fastie, J. Opt. Soc. Am. 51, 1472 (1961A)

## FIGURE CAPTIONS

1. Source-Collector-Detector Geometry.
2. Transmission Curves of Window Materials.
3. Optical Diagram of Ebert Spectrophotometer.
4. Auroral Spectra in the region 1100 to 1540 Å. The top spectrum was obtained in 1965 with presently available optical components. The bottom spectrum was obtained in 1960 with the same observation time from an aurora which was 10 times as bright as the 1965 aurora.
5. The spectrum of NO obtained in the day airglow by Barth <sup>6</sup> in one second of observation time. The top spectrum is calculated, the bottom is the unretouched telemetry trace.
6. Spectrum of the far U. V. day airglow showing four spectra features in the region 1200 to 1360 Å.
7. Altitude profiles of OI 1304 (<sup>3</sup>S-<sup>3</sup>P) day airglow and OI 1356 (<sup>5</sup>S-<sup>3</sup>P) day airglow.
8. Two section baffle for day airglow photometers and spectro-photometers.
9. Diagram of simple field of view limiters.
10. Coronagraph telescope for airglow measurements.
11. Multiple mirror illuminator for enhancing signal from sources of limited area.
12. End view of nine-element multiple mirror system.